

Numerical Studies of Back Reaction Effects in an Analog Model of Cosmological Preheating

Salvatore Butera^{1,*} and Iacopo Carusotto²

¹*School of Physics and Astronomy, University of Glasgow, Glasgow G12 8QQ, United Kingdom*

²*Pitaevskii BEC Center, INO-CNR and Dipartimento di Fisica, Università di Trento, I-38123 Trento, Italy*

 (Received 4 July 2022; revised 25 January 2023; accepted 15 May 2023; published 12 June 2023)

We theoretically propose an atomic Bose-Einstein condensate as an analog model of backreaction effects during the preheating stage of the early Universe. In particular, we address the out-of-equilibrium dynamics where the initially excited inflaton field decays by parametrically exciting the matter fields. We consider a two-dimensional, ring-shaped BEC under a tight transverse confinement whose transverse breathing mode and the Goldstone and dipole excitation branches simulate the inflaton and quantum matter fields, respectively. A strong excitation of the breathing mode leads to an exponentially growing emission of dipole and Goldstone excitations via parametric pair creation: Our numerical simulations of the BEC dynamics show how the associated backreaction effect results not only in an effective friction of the breathing mode, but also in a quick loss of longitudinal spatial coherence of the initially in-phase excitations. Implications of this result on the validity of the usual semiclassical description of backreaction are finally discussed.

DOI: [10.1103/PhysRevLett.130.241501](https://doi.org/10.1103/PhysRevLett.130.241501)

Introduction.—Since Unruh’s pioneering proposal [1], analog models of gravity represent a promising platform where a wide range of effects of quantum fields in curved spacetime can be studied from first principles and potentially find experimental confirmation [2]. A most celebrated achievement was the observation of the analog of Hawking radiation [3,4] emanating from the acoustic horizon in a trans-sonically flowing Bose-Einstein condensates (BECs) of ultracold atoms [5–9]. Analogs of cosmological particle creation effects have also been investigated on the BEC platform both theoretically [10–14] and experimentally [15,16].

While these advances clearly demonstrate the power of the analog gravity program, they all address kinematic, test-field effects of a noninteracting quantum field theory on a predetermined curved spacetime background [17]. The next challenge that stands in front of the analog gravity community is to extend these investigations to the so-called *backreaction* phenomena [18], where the background has its own dynamics and interplays with the quantum field.

A simplest example of such an effect is the radiative friction felt by an accelerated mirror in response to the dynamical Casimir emission [19]. Here, theoretical studies

in a single-mode geometry [20,21] have hinted at an important role of quantum fluctuations of the friction force [22–24]. At an even more idealized level, signatures of backreaction and entanglement effects have been highlighted in trilinear Hamiltonian models in both theory [25] and experiments [26]. Beyond these toy models, a full understanding of quantum features in backreaction effects is of outstanding importance in the case of black hole evaporation under the effect of Hawking emission [27], where one expects that quantum fluctuations may be involved in the so-called information paradox [28]. In the analog model context, first pioneering steps in this direction have been taken in Refs. [29–31].

A seemingly insurmountable hurdle in extending analog gravity toward backreaction effects is posed by the starkly different form of the nonlinear evolution equations, governed by Einstein gravity and the (still unknown) physics of spacetime at the Planck scale on one side and by the (well-controlled) microscopic material dynamics of the analog model on the other side. In this work, we fully acknowledge this difficulty and, as a workaround, we take inspiration from the effective field theory approach [32] and adopt a phenomenological perspective based on the assumption that observable consequences of backreaction at the mesoscopic level such as dissipation, fluctuation, and decoherence result from a coarse-graining process and are, thus, ultimately insensitive to the microscopic details of the interactions [33].

Moving along these lines, we consider in this Letter an analog model of the preheating of the early Universe [34–36] (see also the topical reviews [37–39]). This is the

Published by the American Physical Society under the terms of the Creative Commons Attribution 4.0 International license. Further distribution of this work must maintain attribution to the author(s) and the published article’s title, journal citation, and DOI.

later stage of the inflation, when the inflaton field has ended its slow rolling on the potential plateau and has fallen into the final potential well. The ensuing periodic oscillations around the bottom of the potential well parametrically excite the vacuum fluctuations of the matter fields that are coupled to the inflaton, resulting in an explosive production of matter in the Universe and a corresponding decay of the inflaton oscillations [40,41]. The dynamics of this process has been addressed in previous literature by using simpler single-field models [42,43], as well as more complex configurations and different types of inflaton potentials [44–51].

In our analog model, we simulate this dynamics by using an elongated ring-shaped atomic BEC as experimentally realized in Ref. [16] and first proposed in the context of backreaction studies in Ref. [30]. Under the approximation of a negligible cosmological expansion on the timescale of the preheating stage [37–39], the BEC can be taken to be at rest and stationary so to simulate a flat spacetime. As a key advantage over superconducting [52] or trapped-ion [53] systems, elongated BECs naturally support several different excitation branches [54] that can be used to enrich the analog model by encoding the several different degrees of freedom involved in the cosmological problem at hand. In our proposal, the inflaton field is described by a (gapped) collective transverse breathing mode of the elongated condensate. As it is sketched in Fig. 1, the relatively high-frequency oscillations of the breathing mode then lead to the parametric amplification of zero-point fluctuations in the lower-energy longitudinal (dipole and Goldstone) modes, which encode the matter fields of the cosmological model.

Our theoretical approach is based on *ab initio* numerical simulations of the atomic cloud dynamics via the so-called truncated Wigner approximation (TWA) [56,57]: In contrast to the semiclassical treatment of the breathing mode dynamics in Refs. [30,58], our formalism is able to include the dynamical interplay of the quantum fluctuations in the different modes via the backreaction effects. Differently from Ref. [59], we will not delve here into the physics of thermalization of the generated particles during the successive reheating stage [60–65].

The system.—We consider a dilute two-dimensional gas of mass m atoms at zero temperature, homogeneous along the longitudinal x direction with length L_x and periodic boundary conditions, and trapped in the transverse y direction by an external potential $V_{\text{ext}}(y)$. For numerical convenience, this is taken as harmonic of frequency ω_0 at small y with a hard wall at $y = \pm L_y/2$ on both sides. The many-body Hamiltonian reads [66]

$$\hat{H} = \int d\mathbf{r} \left[\hat{\Psi}^\dagger(\mathbf{r}) \hat{h} \hat{\Psi}(\mathbf{r}) + \frac{U}{2} \hat{\Psi}^\dagger(\mathbf{r}) \hat{\Psi}^\dagger(\mathbf{r}) \hat{\Psi}(\mathbf{r}) \hat{\Psi}(\mathbf{r}) \right], \quad (1)$$

where $\hat{h} \equiv -(\hbar^2/2m)\nabla^2 + V_{\text{ext}}(y)$ is the single-particle Hamiltonian and U is the strength of the zero-range interatomic collisional interaction.

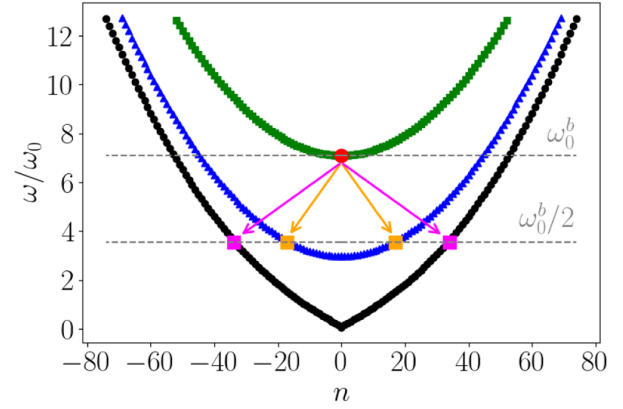


FIG. 1. Bogoliubov spectrum of collective excitations around the ground state. The three curves correspond to modes with zero (Goldstone, black), one (dipole, blue), and two (breathing, green) nodes in the transverse direction. The red circle highlights the transverse breathing mode that is excited at early times to simulate the inflaton oscillations; the yellow (purple) circles highlight the dipole (Goldstone) modes of opposite momenta that are resonantly excited by the parametric processes indicated by the arrows. System parameters: gas of $N = 10^6$ atoms in an integration box of size $L_{x,y}/\ell_0 = 140, 3.54$ in units of the transverse harmonic oscillator length $\ell_0 = \sqrt{\hbar/2m\omega_0}$, with $N_{x,y} = 512, 12$ grid points; equilibrium chemical potential $\mu/\hbar\omega_0 = 2.38$. The independence of our conclusions from the specific numerical parameters is validated in Supplemental Material [55].

At the mean-field level, the quantum field operator $\hat{\Psi}(\mathbf{r})$ is approximated by its classical average $\langle \hat{\Psi}(\mathbf{r}) \rangle \equiv \psi(\mathbf{r})$, whose evolution follows the so-called Gross-Pitaevskii (GP) equation [54]

$$i\hbar \frac{\partial \psi}{\partial t} = -\frac{\hbar^2}{2m} \nabla^2 \psi + U|\psi|^2 \psi. \quad (2)$$

The quantum dynamics of small excitations on top of a stationary ground-state BEC can then be described at second order in the fluctuation amplitude around the mean field by the Bogoliubov theory [67]. The spectrum $\{\omega_n^r\}$ of the collective Bogoliubov modes and the corresponding eigenfunctions $\{u_n^r, v_n^r\}$ are calculated by diagonalizing the Bogoliubov operator [67]

$$\mathcal{L}_{\text{Bog}}[\psi, \psi^*] \equiv \begin{pmatrix} \hat{H}_{\text{GP}} + UQ|\psi|^2Q & UQ\psi^2Q^* \\ -UQ^*\psi^{*2}Q & -[\hat{H}_{\text{GP}} + UQ|\psi|^2Q] \end{pmatrix}, \quad (3)$$

where the operator $Q \equiv \mathbb{I} - |\psi\rangle\langle\psi|$ projects orthogonally to the single-particle condensate wave function ψ , $\hat{H}_{\text{GP}} \equiv \hat{h} + U|\psi|^2 - \mu$ is the GP Hamiltonian, and μ is the chemical potential.

For each mode, the integer-valued subscript n and the superscript $r = g, d, b, \dots$, respectively, identify the

longitudinal wave vector $k = 2\pi n/L_x$ and the different excitation branches, labeled by the number of transverse nodes in the wave function (g = Goldstone, zero nodes; d = dipole, one node; b = breathing, two nodes). As a concrete example, the dispersion of the Goldstone, dipole, and breathing branches for the system parameters used throughout this work is shown in Fig. 1, together with the basic parametric emission processes. Thanks to the anharmonicity of the transverse confinement potential, parametric emission can occur in both g and d branches.

The usual way of understanding the parametric emission of Bogoliubov quanta in time-dependent condensates consists of generalizing the Bogoliubov theory to the case of a time-dependent background $\psi(t)$. While this approach well describes both spontaneous and stimulated (and, thus, exponentially growing) parametric emission processes, it implicitly assumes that the background dynamics encoded in the time-dependent Bogoliubov operator $\mathcal{L}_{\text{Bog}}(t) = \mathcal{L}_{\text{Bog}}[\psi(t), \psi^*(t)]$ is not affected by the parametric emission. In order to capture the backreaction effect of the parametric emission onto the breathing mode oscillations and, in particular, its quantum fluctuations, we need to go beyond this mean-field-like picture.

Simulation method.—In our alternative picture, the parametric emission can be seen as the conversion of b -branch Bogoliubov quanta of the ground-state condensate into pairs of quanta in either the g or the d branches, mediated by nonlinear terms that go beyond the quadratic Bogoliubov Hamiltonian and describe interactions and interconversion between the Bogoliubov modes, e.g., the so-called Beliaev-Landau damping processes [68–71].

Beyond this perturbative picture, a simulation of the full nonlinear dynamics of the atomic gas including nonperturbative interactions between Bogoliubov quasiparticles can be numerically carried out within the TWA [56,57]. The basic idea of TWA is to describe the quantum field operator $\hat{\Psi}(\mathbf{r})$ in terms of a suitably distributed stochastic classical field $\psi(\mathbf{r})$, whose stochastic averages (indicated as $\langle \cdot \rangle_W$ in what follows) provide quantum expectation values of symmetrically ordered observables. For conservative systems like atomic gases, quantum noise is encoded in the initial state $\psi(\mathbf{r}, t=0)$ of the classical field, which then follows a deterministic time evolution according to the standard GP equation [Eq. (2)]. Interestingly, similar classical field approaches are of current use also in the cosmological literature [61].

In the context of analog models, the TWA has been widely exploited to study quantum field effects at the test-field level such as analogs of cosmological particle creation [12] and of Hawking radiation [6] and has recently started to be pushed beyond this regime [30]. The validity of the TWA for our purposes is supported by previous work on backreaction effects in few-mode systems [24], where TWA turned out to be a good approximation provided the population of all relevant modes is macroscopic.

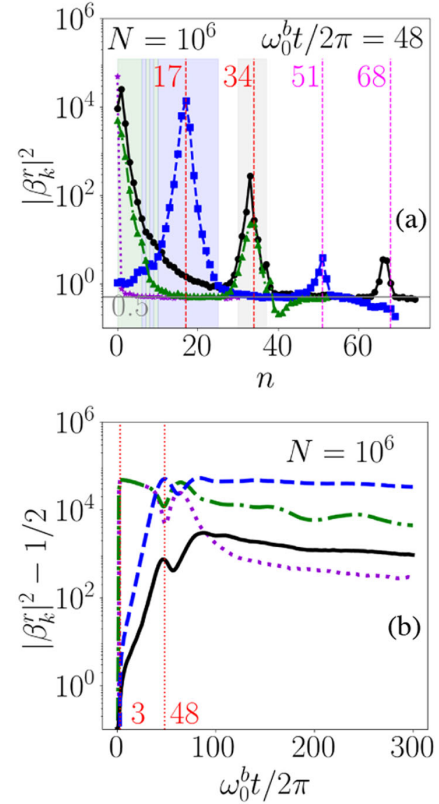


FIG. 2. Numerical results of the TWA simulations. Stochastic averages are based on a sample of $\mathcal{N}_r = 1000$ independent realization. (a) Momentum distribution of the population in the Bogoliubov modes at time $\omega_0^b t/2\pi = 48$. The dot-dashed green, dashed blue, and solid black lines correspond to the breathing, dipole, and Goldstone branches, respectively. The dotted violet line shows the population in the breathing mode immediately after the excitation sequence. (b) Time evolution of the integrated population in the breathing, dipole, and Goldstone branches over the regions indicated by the shading in (a). The same color code as in (a). The dotted violet line shows the time evolution of the population in the single breathing mode at $k = 0$.

Figure 2 shows how this condition is well verified in our calculations for the resonant modes on the breathing, dipole, and Goldstone branches.

In particular, we consider the gas to be initially in its ground state. Within the TWA, the classical field distribution corresponding to the ground state is constructed as the sum of the GP ground state $\psi_0(\mathbf{r})$, plus a Gaussian stochastic component that accounts for the zero-point fluctuations of the Bogoliubov modes [56,57]:

$$\psi(\mathbf{r}, t=0) = \psi_0(\mathbf{r}) + \sum_{n,r} [\beta_n^r u_n^r(\mathbf{r}) + \beta_n^{r*} v_n^{r*}(\mathbf{r})]. \quad (4)$$

Here, the β_n^r coefficients for each (positive-norm) n, r Bogoliubov mode are independent, zero-mean, Gaussian random variables with $\langle \beta_k^2 \rangle = 0$ and $\langle |\beta_k|^2 \rangle = 1/2$. In our simulations, a sample of $\mathcal{N}_r = 1000$ independent

realizations of the classical field is used, with an initial distribution drawn according to Eq. (4).

Numerical results.—In Fig. 2, we illustrate the evolution of the population in the different Bogoliubov modes, $n_n^r(t) + 1/2 \equiv \langle (\hat{b}_n^r)^\dagger \hat{b}_n^r + \hat{b}_n^r (\hat{b}_n^r)^\dagger \rangle / 2 = \langle |\beta_n^r(t)|^2 \rangle_w$ as a function of time. At the initial time $t = 0$, the system is prepared in the Bogoliubov vacuum and the modes host only zero-point fluctuations, $n_n^r(t = 0) = 0$. Around a time $\omega_0 t_0 / 2\pi = 2$, we impart a short modulation of the trapping frequency, $\omega_0(t) / \omega_0 = 1 + A e^{-(t-t_0)^2 / 2\sigma_t^2}$ of amplitude A and duration σ_t so to excite the spatially uniform $k = 0$ transverse breathing mode of the condensate (red circle in Fig. 1). This excitation is visible as a marked $k = 0$ peak in the momentum-resolved occupation of the b modes right after the kick [purple dotted line in Fig. 2(a)].

Afterward, the nonlinear coupling between the b and g, d modes makes the vacuum fluctuations in the dipole and Goldstone modes get parametrically excited by the oscillations in the transverse direction. Because of the ring configuration here considered, momentum in the longitudinal direction is conserved and the parametric down-conversion process involves pairs of particles with opposite momenta as indicated by arrows in Fig. 1. Energy conservation makes the parametric processes to be most effective into the Goldstone and dipole modes of frequency $\omega_{\text{res}}^{g,d} = \omega_0^b / 2$ for which the parametric emission is resonant with the breathing mode oscillations at ω_0^b that are driving it, as shown in the momentum distributions in Fig. 2(a).

Given the bosonic nature of the Bogoliubov modes, the parametric emission starts from zero-point quantum fluctuations but then gets self-stimulated as more and more population is created, leading to an exponential growth of the population in the resonant modes. This behavior is apparent in the black solid and blue dashed lines in Fig. 2(b), which display the evolution of the integrated population within the integration windows indicated by the shaded areas in Fig. 2(a). This exponential growth is analogous of the explosive production of matter that takes place during the preheating of the early Universe.

At late times, nonlinear and saturation effects start to dominate the dynamics [60–62,65]. Nonlinear effects are visible in the appearance of harmonic peaks in the momentum distributions [30,62,72] as well as an increased width of all peaks. Self-interaction, scattering, and thermalization processes within the Goldstone and dipole branches are responsible for these effects: While they are of great interest as an analog model [59] of cosmological reheating [60–62,65], a detailed study goes beyond the purpose of this work and is postponed to future work.

Here, we rather focus on the dynamics of the breathing mode b during the earlier preheating stage. As a most important feature, in Fig. 2(b), we see a marked drop in the integrated population in the breathing b branch (green dashed line) as soon as the populations in the g, d modes reach a value comparable to the one in the b mode and

backreaction starts exerting a sizable effective friction onto the b mode. Interestingly, such a damping is not purely monotonic, but energy gets at least partially exchanged between the modes. This intermediate-time damped-oscillatory phenomenology is qualitatively similar to the one predicted in Refs. [21,24] for the backreaction effect of dynamical Casimir processes in a single-mode cavity configuration, with interesting new features stemming from the many-mode nature of our system that we are now going to highlight. The crucial role of quantum fluctuations in the dynamics is confirmed by the additional simulations reported in Supplemental Material [55], which highlight a stronger friction in a stronger interacting BEC.

Local observables.—One may be concerned that the very concept of Bogoliubov modes may cease being well defined in a regime where nonlinear effects are playing a major role. To circumvent this objection, we complement the modewise analysis in Fig. 2 with a study of real-space quantities. Specifically, we consider the x -dependent transverse cloud size

$$w(x, t) \equiv \frac{\int_0^{L_y} dy |\psi(\mathbf{r}, t)|^2 y^2}{\int_0^{L_y} dy |\psi(\mathbf{r}, t)|^2} \quad (5)$$

and the spatial correlation function

$$C_w(X; t) \equiv \left\langle \frac{\delta w(x, t) \delta w(x + X, t)}{\bar{w}^2(0)} \right\rangle_w \quad (6)$$

of its fluctuations $\delta w(x, t) = w(x, t) - \bar{w}(0)$ from the initial value $\bar{w}(0)$ of its spatial average $\bar{w}(t) \equiv L_x^{-1} \int_0^{L_x} dx w(x, t)$ at $t = 0$.

The time evolution of $C_w(X; t)$ is illustrated in the left panel in Fig. 3. Right after the initial kick around $\omega_0^b t = 2$, the breathing mode oscillates coherently with a uniform amplitude throughout the cloud, and the correlation function is large and constant. Then, not only does the overall magnitude of C_w decrease as a signature of backreaction-induced damping, but spatial coherence is also lost at an even faster rate [73]. As one can see in the cuts in the middle panel, at late times the correlation function maintains a sizable value only in the sharp peak around $X = 0$: Referring specifically to the $\omega_0^b t = 150$ curve, this indicates that the intensity of the b oscillations, encoded in $C_w(0; t)$, has dropped by a factor around 3 but has almost completely lost its spatial decoherence as shown by the negligible value $C_w(L/2; t) \approx 0$. A further visualization of this effect is available in the right panel in Fig. 3, which highlights the much faster decrease of the long-distance coherence $C_w(L/2; t)$ (blue dashed line) and a relative stabilization of the oscillation intensity (black solid line).

A momentum-space signature of this effect is visible as a marked broadening of the k -space breathing mode distribution as time proceeds [green line in Fig. 2(a)], whose

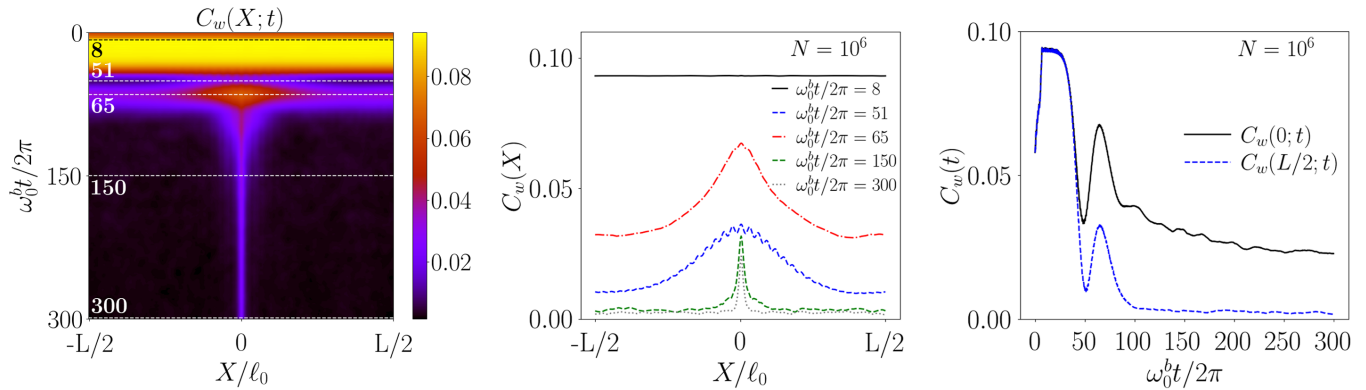


FIG. 3. Left panel: color plot of the time evolution of the spatial correlation function $C_w(X;t)$ of the transverse size of the condensate. Cuts at different times (indicated by the horizontal dashed lines) are shown in the middle panel. Right panel: time evolution of the spatial correlation function for coincident $C_w(0;t)$ and opposite $C_w(L/2;t)$ points around the ring. The same system and simulation parameters as in Figs. 1 and 2.

large momentum width corresponds to the short real-space coherence length. This population redistribution from the single initial $k = 0$ mode into a wider band of modes is further visible by comparing the purple dashed and green dot-dashed curves in Fig. 2(b), whose time evolution recovers the one of the C_w at $X = L/2$ and at $X = 0$ shown in the blue and black curves of the right panel in Fig. 3.

These results are the most exciting prediction of our numerics: While traditional semiclassical models of backreaction in gravitation and cosmology include the effect of the quantum emission within a mean-field theory via its average contribution to the energy-stress tensor to be included in the Einstein equations [30,33,74], this figure shows how the large fluctuations of the two-mode-squeezed-like state of the emitted g , d fields directly transfer into an analogous fluctuation of the backreaction-induced friction force. Evidence of the nonlinear nature of the backreaction coupling is offered by the non-Gaussian shape of the Wigner distributions shown in Supplemental Material [55]. While the possibility of such an effect was implicitly mentioned in Ref. [60] and preliminary evidence was already visible in our single-mode calculations [24], our results here show how the consequences of the friction-induced decoherence are qualitatively dramatic in a spatially extended multimode geometry.

Conclusions.—In this work, we have theoretically considered an atomic Bose-Einstein condensate as an analog model of the nonlinear nonequilibrium dynamics of the inflaton field in the preheating stage of the early Universe. Our numerical results predict a crucial role of quantum fluctuations in the backreaction effect of particle production onto the inflaton field: Not only does the emission of dipole and Goldstone excitations lead to an effective damping of the breathing mode as predicted by a semiclassical picture, but it is also responsible for a quick decoherence of its initially in-phase excitation. The generality of the microscopic processes underlying our numerically observed results points at the

importance of going beyond semiclassical approaches [74,75] and including quantum fluctuation features in the description of backreaction phenomena in gravitation and cosmology. Future work will extend the study to the elusive backreaction phenomena that are responsible for black hole evaporation under the effect of Hawking emission.

Continuous support from Massimiliano Rinaldi on cosmological issues is most appreciated, as well as enlightening discussions with Stephen Barnett, Miles Blencowe, Bei-Lok Hu, and Renaud Parentani. S.B. acknowledges funding from the Leverhulme Trust Grant No. ECF-2019-461 and from University of Glasgow via the Lord Kelvin/Adam Smith (LKAS) Leadership Fellowship. I.C. acknowledges support from the European Union Horizon 2020 research and innovation program under Grant Agreement No. 820392 (PhoQuS) and from the Provincia Autonoma di Trento.

*Corresponding author.

salvatore.butera@glasgow.ac.uk

- [1] W. G. Unruh, *Phys. Rev. Lett.* **46**, 1351 (1981).
- [2] C. Barceló, S. Liberati, and M. Visser, *Living Rev. Relativity* **14**, 3 (2011).
- [3] S. W. Hawking, *Nature (London)* **248**, 30 (1974).
- [4] S. W. Hawking, *Commun. Math. Phys.* **43**, 199 (1975).
- [5] L. J. Garay, J. R. Anglin, J. I. Cirac, and P. Zoller, *Phys. Rev. Lett.* **85**, 4643 (2000).
- [6] I. Carusotto, S. Fagnocchi, A. Recati, R. Balbinot, and A. Fabbri, *New J. Phys.* **10**, 103001 (2008).
- [7] J. Steinhauer, *Nat. Phys.* **12**, 959 (2016).
- [8] J. de Nova, K. Golubkov, V. Kolobov, and J. Steinhauer, *Nature (London)* **569**, 688 (2019).
- [9] V. Kolobov, K. Golubkov, J. de Nova, and J. Steinhauer, *Nat. Phys.* **17**, 362 (2021).
- [10] P. O. Fedichev and U. R. Fischer, *Phys. Rev. A* **69**, 033602 (2004).

- [11] U. R. Fischer and R. Schützhold, *Phys. Rev. A* **70**, 063615 (2004).
- [12] P. Jain, S. Weinfurter, M. Visser, and C. W. Gardiner, *Phys. Rev. A* **76**, 033616 (2007).
- [13] I. Carusotto, R. Balbinot, A. Fabbri, and A. Recati, *Eur. Phys. J. D* **56**, 391 (2010).
- [14] S. Butera and I. Carusotto, *Phys. Rev. D* **104**, 083503 (2021).
- [15] C.-L. Hung, V. Gurarie, and C. Chin, *Science* **341**, 1213 (2013).
- [16] S. Eckel, A. Kumar, T. Jacobson, I. B. Spielman, and G. K. Campbell, *Phys. Rev. X* **8**, 021021 (2018).
- [17] N. D. Birrell and P. C. W. Davies, *Quantum Fields in Curved Space*, Cambridge Monographs on Mathematical Physics (Cambridge University Press, Cambridge, England, 1984).
- [18] B.-L. Hu and E. Verdaguer, *Semiclassical and Stochastic Gravity: Quantum Field Effects on Curved Spacetime*, Cambridge Monographs on Mathematical Physics (Cambridge University Press, Cambridge, England, 2020).
- [19] M. Kardar and R. Golestanian, *Rev. Mod. Phys.* **71**, 1233 (1999).
- [20] V. Macrì, A. Ridolfo, O. Di Stefano, A. F. Kockum, F. Nori, and S. Savasta, *Phys. Rev. X* **8**, 011031 (2018).
- [21] S. Butera and I. Carusotto, *Phys. Rev. A* **99**, 053815 (2019).
- [22] D. A. R. Dalvit and P. A. Maia Neto, *Phys. Rev. Lett.* **84**, 798 (2000).
- [23] P. A. Maia Neto and D. A. R. Dalvit, *Phys. Rev. A* **62**, 042103 (2000).
- [24] S. Butera and I. Carusotto, *Europhys. Lett.* **128**, 24002 (2019).
- [25] P. D. Nation and M. P. Blencowe, *New J. Phys.* **12**, 095013 (2010).
- [26] S. Ding, G. Maslennikov, R. Hablützel, and D. Matsukevich, *Phys. Rev. Lett.* **121**, 130502 (2018).
- [27] A. Fabbri and J. Navarro-Salas, *Modeling Black Hole Evaporation* (World Scientific, Singapore, 2005).
- [28] J. Maldacena, *Nat. Rev. Phys.* **2**, 123 (2020).
- [29] J. R. M. de Nova, S. Finazzi, and I. Carusotto, *Phys. Rev. A* **94**, 043616 (2016).
- [30] S. Robertson, F. Michel, and R. Parentani, *Phys. Rev. D* **98**, 056003 (2018).
- [31] S. Patrick, H. Goodhew, C. Gooding, and S. Weinfurter, *Phys. Rev. Lett.* **126**, 041105 (2021).
- [32] J. Bain, *Stud. Hist. Phil. Mod. Phys.* **44**, 338 (2013).
- [33] B. Hu, *Int. J. Theor. Phys.* **44**, 1785 (2005).
- [34] A. Dolgov and D. Kirilova, *Yad. Fiz.* **51**, 273 (1990).
- [35] A. Dolgov and D. Kirilova, *Sov. J. Nucl. Phys.* **51**, 172 (1990).
- [36] J. H. Traschen and R. H. Brandenberger, *Phys. Rev. D* **42**, 2491 (1990).
- [37] B. A. Bassett, S. Tsujikawa, and D. Wands, *Rev. Mod. Phys.* **78**, 537 (2006).
- [38] R. Allahverdi, R. Brandenberger, F.-Y. Cyr-Racine, and A. Mazumdar, *Annu. Rev. Nucl. Part. Sci.* **60**, 27 (2010).
- [39] M. A. Amin, M. P. Hertzberg, D. I. Kaiser, and J. Karouby, *Int. J. Mod. Phys. D* **24**, 1530003 (2015).
- [40] L. Kofman, A. Linde, and A. A. Starobinsky, *Phys. Rev. Lett.* **73**, 3195 (1994).
- [41] Y. Shtanov, J. Traschen, and R. Brandenberger, *Phys. Rev. D* **51**, 5438 (1995).
- [42] S. Y. Khlebnikov and I. I. Tkachev, *Phys. Rev. Lett.* **77**, 219 (1996).
- [43] D. T. Son, *Phys. Rev. D* **54**, 3745 (1996).
- [44] R. Allahverdi and B. A. Campbell, *Phys. Lett. B* **395**, 169 (1997).
- [45] P. B. Greene, L. Kofman, A. Linde, and A. A. Starobinsky, *Phys. Rev. D* **56**, 6175 (1997).
- [46] G. Felder, J. García-Bellido, P. B. Greene, L. Kofman, A. Linde, and I. Tkachev, *Phys. Rev. Lett.* **87**, 011601 (2001).
- [47] G. Felder, L. Kofman, and A. Linde, *Phys. Rev. D* **64**, 123517 (2001).
- [48] M. A. Amin, R. Easter, and H. Finkel, *J. Cosmol. Astropart. Phys.* **12** (2010) 001.
- [49] M. A. Amin, R. Easter, H. Finkel, R. Flauger, and M. P. Hertzberg, *Phys. Rev. Lett.* **108**, 241302 (2012).
- [50] K. D. Lozanov and M. A. Amin, *Phys. Rev. D* **97**, 023533 (2018).
- [51] K. D. Lozanov and M. A. Amin, *Phys. Rev. D* **99**, 123504 (2019).
- [52] P. D. Nation, M. P. Blencowe, A. J. Rimberg, and E. Buks, *Phys. Rev. Lett.* **103**, 087004 (2009).
- [53] C. Fey, T. Schaez, and R. Schützhold, *Phys. Rev. A* **98**, 033407 (2018).
- [54] L. Pitaevskii and S. Stringari, *Bose-Einstein Condensation and Superfluidity*, International Series of Monographs on Physics (Oxford University Press, New York, 2016).
- [55] See Supplemental Material at <http://link.aps.org/supplemental/10.1103/PhysRevLett.130.241501> for similar results as the ones shown in the main text, with different number of particles and sizes of the system, as well as different numbers of grid-points in the numerical grid that we use in our simulations. These results demonstrate that the physics we observe is independent from the specific values of the physical/numerical parameters.
- [56] M. J. Steel, M. K. Olsen, L. I. Plimak, P. D. Drummond, S. M. Tan, M. J. Collett, D. F. Walls, and R. Graham, *Phys. Rev. A* **58**, 4824 (1998).
- [57] A. Sinatra, C. Lobo, and Y. Castin, *Phys. Rev. Lett.* **87**, 210404 (2001).
- [58] T. V. Zache, V. Kasper, and J. Berges, *Phys. Rev. A* **95**, 063629 (2017).
- [59] A. Chatrchyan, K. T. Geier, M. K. Oberthaler, J. Berges, and P. Hauke, *Phys. Rev. A* **104**, 023302 (2021).
- [60] L. Kofman, A. Linde, and A. A. Starobinsky, *Phys. Rev. D* **56**, 3258 (1997).
- [61] T. Prokopec and T. G. Roos, *Phys. Rev. D* **55**, 3768 (1997).
- [62] R. Micha and I. I. Tkachev, *Phys. Rev. Lett.* **90**, 121301 (2003).
- [63] D. Podolsky, G. N. Felder, L. Kofman, and M. Peloso, *Phys. Rev. D* **73**, 023501 (2006).
- [64] G. Felder and L. Kofman, *Phys. Rev. D* **63**, 103503 (2001).
- [65] D. G. Figueroa and F. Torrentí, *J. Cosmol. Astropart. Phys.* **02** (2017) 001.
- [66] F. Dalfovo, S. Giorgini, L. Pitaevskii, and S. Stringari, *Rev. Mod. Phys.* **71**, 463 (1999).
- [67] Y. Castin and R. Dum, *Phys. Rev. A* **57**, 3008 (1998).
- [68] L. Pitaevskii and S. Stringari, *Phys. Lett. A* **235**, 398 (1997).
- [69] W. V. Liu, *Phys. Rev. Lett.* **79**, 4056 (1997).

- [70] S. Giorgini, *Phys. Rev. A* **57**, 2949 (1998).
- [71] P. O. Fedichev and G. V. Shlyapnikov, *Phys. Rev. A* **58**, 3146 (1998).
- [72] V. S. Barroso, A. Geelmuyden, Z. Fifer, S. Erne, A. Avgoustidis, R. J. A. Hill, and S. Weinfurter, [arXiv:2207.02199](https://arxiv.org/abs/2207.02199).
- [73] G. N. Felder and L. Kofman, *Phys. Rev. D* **75**, 043518 (2007).
- [74] S. Pla, I. M. Newsome, R. S. Link, P. R. Anderson, and J. Navarro-Salas, *Phys. Rev. D* **103**, 105003 (2021).
- [75] P. R. Anderson, C. Molina-París, and D. H. Sanders, *Phys. Rev. D* **92**, 083522 (2015).